The Henryk Niewodniczański
INSTITUTE OF NUCLEAR PHYSICS
Polish Academy of Sciences
ul. Radzikowskiego 152, 31-342 Kraków, Poland

www.ifj.edu.pl/publ/reports/2014/

Kraków, 2014

Report No. 2073/AP

Assumptions for the design of a neutron pinhole camera dedicated to the PF-24 device

M. Scholz, J. Bielecki, A. Wójcik-Gargula, U. Wiącek, K. Drozdowicz,
A. Igielski, A. Kulińska, G. Tracz, U. Woźnicka

The work has been performed within the framework of the strategic research project "Technologies supporting the development of safe nuclear power engineering" financed by the National Centre for Research and Development (NCBiR). Research task „Research and development of techniques for the controlled thermonuclear fusion", Contract No. SP/J/2/143234/11.

Abstract

The report presents main assumptions on the design of the neutron pinhole camera dedicated to the PF-24 (Plasma Focus) device. The pinhole camera will be used for the investigation of the spatial and temporal distributions of DD neutrons from the PF-24 source. It makes use of principles of the optical geometry adopted for neutron imaging. In the report the evaluation of pinhole geometrical layout has been made on the basis of principles of the geometrical optics. A further optimization of the pinhole geometry has been carried out by means of neutron transport calculations (the MCNP code). The main aim of this report is to provide information on technical solutions for the neutron pinhole.

1. Introduction

Plasma-Focus (PF) device belongs to the family of the dynamic, non-cylindrical Z-pinches and is based on a pulsed high-current discharge between two coaxial electrodes placed in a working gas, usually deuterium. Over the last years the interest in PF devices has increased because they are one of the most efficient sources of pulsed fusion neutron emission. An important feature of the neutron source in the PF is its location and the evolution in time. This is due to the fact that measurements of the spatial distribution of the neutron emission from the PF at a time during one discharge can be used to determine the spatial and temporal distribution of the nuclear fusion reaction rate in the PF.

Thus, space and time resolved measurements of the PF neutron source can give information about relevant production processes, and allow a more reliable discussion of the character of the deuterium fusion in the PF pinch gathered through other diagnostics.

Suggestions regarding the position of the emission of neutrons in the PF presented in [1] and [2] showed different position and size of the neutron source in the PF. These differences may have resulted from the fact that the registration presented in the papers were carried out during several PF discharges. Later, the first measurements of the position and size of the neutron source in one PF discharge were reported in [3] and [4].

In the paper the project design of the new time-resolved neutron pinhole camera for studying pinch plasma in the PF24, based on a new possibility related to detection techniques and neutron transport calculation, is described. Additionally, in the study of the dynamics of neutron emission, the fact that the intensity of the 50 ns long DD neutron pulse is not very high (10^8 – 10^{10} neutrons per shot) must be taken into account. Thus, a high detection efficiency is required.

2. Pinhole camera optics

A neutron pinhole camera imaging is based on the rectilinear propagation of the radiation as like in the standard optical pinhole. A small circular “pinhole” is an absorbing box, located at a distance x from the object. The “pinhole” produces an inverted image on the screen at a given distance x' (Fig. 1). The magnification of the image is:

$$p = \frac{x'}{x} = \frac{y'}{y}, \tag{1}$$

where x and x' refer to the object-to-pinhole and pinhole-to-image distance, respectively, and y and y' are object and image sizes, respectively.

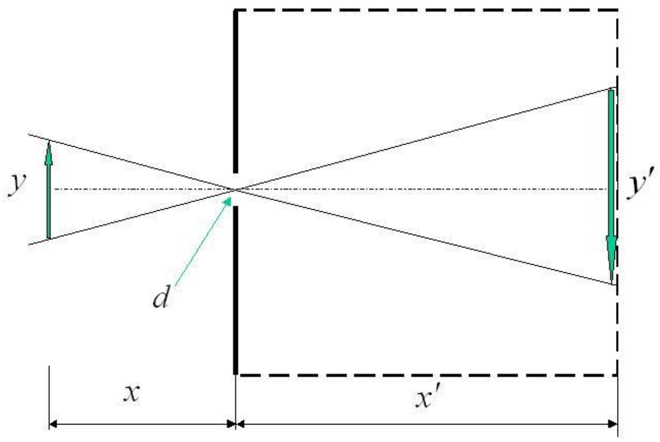

Fig. 1. Scheme of a pinhole camera.

Due to a finite size of the pinhole, a point object is projected as a circular image with a diameter given by:

$$D = d\,\frac{x + x'}{x} = d(1 + p), \tag{2}$$

where d is a pinhole diameter and D is a circular image diameter (see Fig. 2).

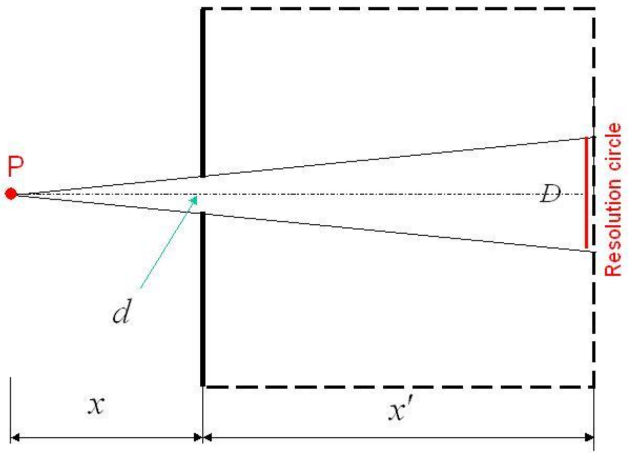

Fig. 2. Resolution circle of the pinhole camera.

The resolution circle can be very small by making the pinhole small and thus the image is very sharp. Diffraction effects are the limit of the pinhole diameter for the optical camera but for the neutron imaging the minimum useful diameter is determined by the neutron source intensity.

The spatial resolution R between two point objects is defined as the distance between them whose resolution circles D on the image plane are tangential (see Fig. 3).

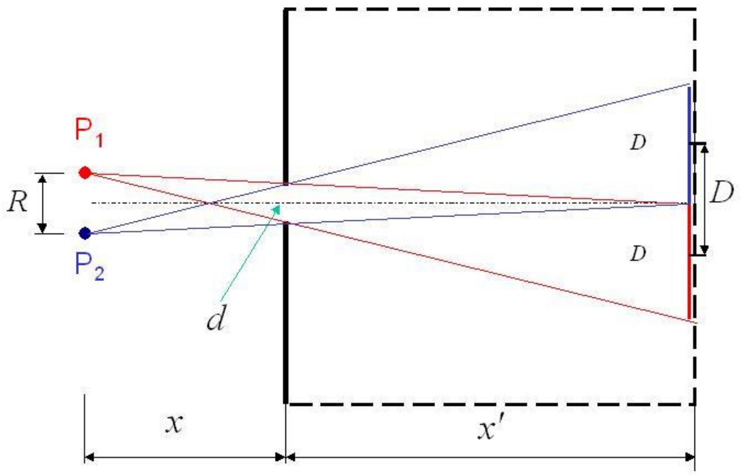

Fig. 3. Space resolution of the pinhole camera.

The resolution distance R is given by:

$$R = 2D\frac{x}{x'} = \frac{1}{2}2d(1+p)\frac{1}{p} = d(1+\frac{1}{p})\,. \tag{3}$$

In the project a single circular pinhole is considered although another pinhole configuration can be chosen. The geometrical considerations presented above are used to calculate the neutron fluence at the image plane. The neutron fluence determines the detection efficiency required for a given total neutron yield Y_n from the PF-24 device. The image neutron fluence is defined as:

$$f = \frac{N_n}{S}\,, \tag{4}$$

where N_n is the number of neutrons passing through the pinhole, S is the image area. For a given total yield of neutrons Y_n emitted from the PF, the image fluence f is determined by:

$$f = \frac{N_n}{S} = \frac{Y_n \dfrac{d^2}{4\pi x^2}}{S}\,. \tag{5}$$

In order to find the experimental conditions which give a resolution distance and other geometrical factors, the experimental set-up of the PF-24 device should be considered.

3. PF-24 device and the experimental set-up

The medium scale PF-24 facility in IFJ PAN consists of the following main units (Fig. 4):

- condenser bank and pulsed electrical power circuit with a collector and low-inductance cables,
- pumping and gas systems consisting of a vacuum chamber, coaxial electrodes and a gas handling system.

Fig.4. General view of the PF-24 device in IFJ PAN.

The electrical energy is transferred to the collector and electrodes by means of low-inductance cables. The vacuum chamber, which surrounds the electrodes, has the following dimensions: 360 mm in diameter and 400 mm in length. Two coaxial electrodes are shown on Fig. 5. The outer electrode (cathode) consists of 16 stainless steel rods with 12 mm in diameter. The outer electrode (OE) radius is the distance between the axis and the centre of outer cathode bar R_{OE} = 55 mm. The copper central electrode (CE) radius is R_{CE} = 30.5 mm. The CE length is 165 mm. The cylindrical alumina insulator sits on the CE and the main part of the insulator extends 32.5 mm along the CE into the vacuum chamber. The insulator prescribes the shape of the initial current sheet between the CE and the back plate of the OE.

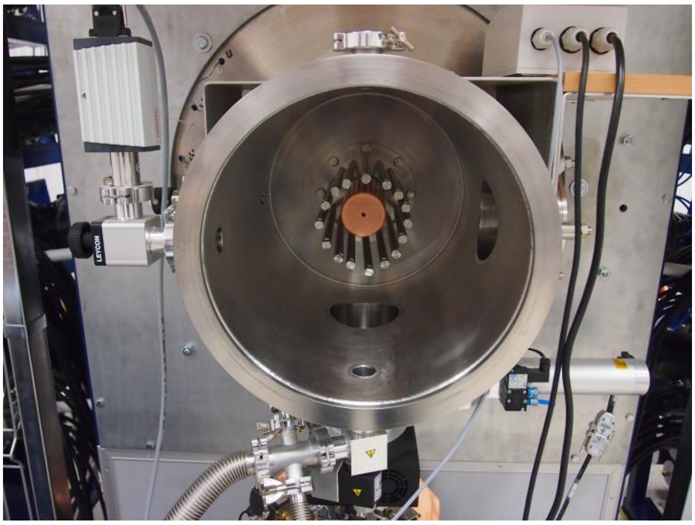

Fig. 5. Geometry of electrodes of the PF-24 device.

The condenser bank of capacitance of 116 μF is charged to voltage ranging between 16 – 40 kV, which corresponds to discharge energies ranging from 15 kJ to 93 kJ. For this range of energy, the total neutron yield range is based on the scaling laws [5], $Y_n = 10^7 \cdot W^2$, where W is energy in kJ, and can be estimated at $10^9 - 10^{11}$. In addition, it can be assumed that the area of neutron emission corresponds to the plasma column created in PF-24. In the PF devices whose energy level of the condenser bank reaches about 100 kJ, the typical plasma column has a length of 3 – 5 cm and a diameter of about 0.8 – 1.2 cm (see Fig. 6).

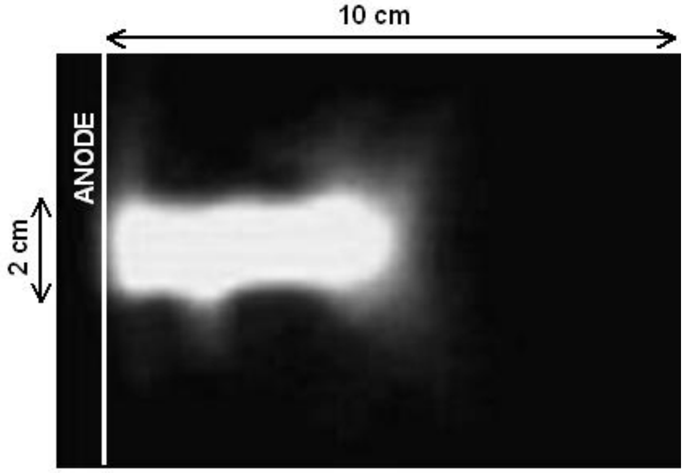

Fig. 6. Example of soft X ray image of a pinch 10 ns before the maximum compression. An exposure time is 2 ns [6].

Based on the above considerations, a typical size of the neutron source in experiments at PF 24 can be assumed as 3 – 5 cm for the length and 0.8 – 1.5 cm in diameter of the source. Hence, the field of view of the pinhole camera should cover an area of the size of $0 \le z \le 5$ cm and $0 \le r \le 1.5$ cm. The object-to-image magnification ratio has been chosen as 1:1, which means that magnification factor is 1. Geometrical dimensions of a single scintillator have been selected as follows:

- 0.5 cm width to cover the most dense region in the plasma column (the diameter of the column up to 1 cm);
- 5 cm depth to ensure a reasonable compromise between the detector efficiency and the neutron cross-talk between the neighbouring detectors;
- 0.5 cm height defines a resolution of the distance R, Eq.(3), and is a compromise between resolution, number of detectors to be used, total length to be investigated and the neutron fluence incident upon each scintillator.

Assuming that the resolution distance R is defined by the scintillator width and height (which is 0.5 cm) the pinhole diameter can be determined for magnification factor $p = 1$ as to be less than $d = 0.25$ cm.

Substituting into Eq.(5) the following numbers: $Y_n = 10^9 \div 10^{11}$ neutrons/discharge, $d \le 0.25$ cm, $S = 0.5 \times 5$ cm^2, the relation between image fluency and the distance of the pinhole from the pinch is determined by:

$$f \cong 1.27(10^6 \div 10^8)\frac{1}{x^2} , \tag{6}$$

where f is in neutron/cm^2 and $d = 0.2$ cm was used.

A minimum of 100 neutrons/detector at the image plane is assumed in order to get a reasonable statistics with an efficient detector. Using formula (6), the number of neutrons incident on the detector as a function of distance of the pinhole from the pinch can be determined, assuming that the area of the scintillator is $0.5\times0.5 = 0.25$ cm^2 (see Fig. 7).

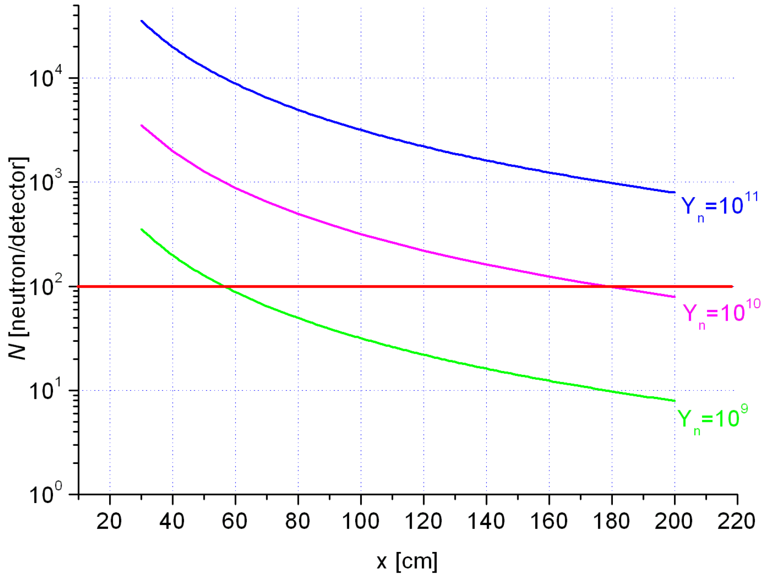

Fig.7. Number of neutrons incident onto the detector as a function of distance of the pinhole from the pinch for different neutron yields of PF-24. Red line corresponds to 100 neutrons/detector.

Fig. 7 shows that the distance between the source and the pinhole for the neutron yield on a level of 10^9 should be less than 50 cm. This must be adjusted down providing for any neutron attenuation in the vacuum chamber and shielding.

4. Shielding and pinhole design

While using principles of geometrical optics for fast neutrons it should be stressed that the construction of the neutron pinhole camera is drastically different from the optical one. In particular, completely different shielding and collimation concepts must be applied due to a specific nature of the neutron propagation in the matter. Thus this requires the pinhole to be several neutron mean free paths (in its material) long in order to get the required collimation of the neutrons. Moreover, the camera walls should be a very good absorber of the neutrons.

The consideration made in the previous section has shown that the neutron pinhole camera is located near the pinch column (a neutron source). Therefore, the detectors must be surrounded by a specific shell walls. This type of walls are necessary to reduce background substantially below the direct signals. It means, that only the narrowly collimated line of sight allows for the rectilinear propagation of neutrons from source to detector.

A geometrical layout of the pinhole and shielding regions is shown in Fig. 8. The pinhole region extends out into two anti-scattering cones, one in front of the defining pinhole element and the other outside. A neutron scattered from the wall of the front cone cannot get through the pinhole unless it makes additional scatter. The collimator setup of the pinhole camera will be made of copper.

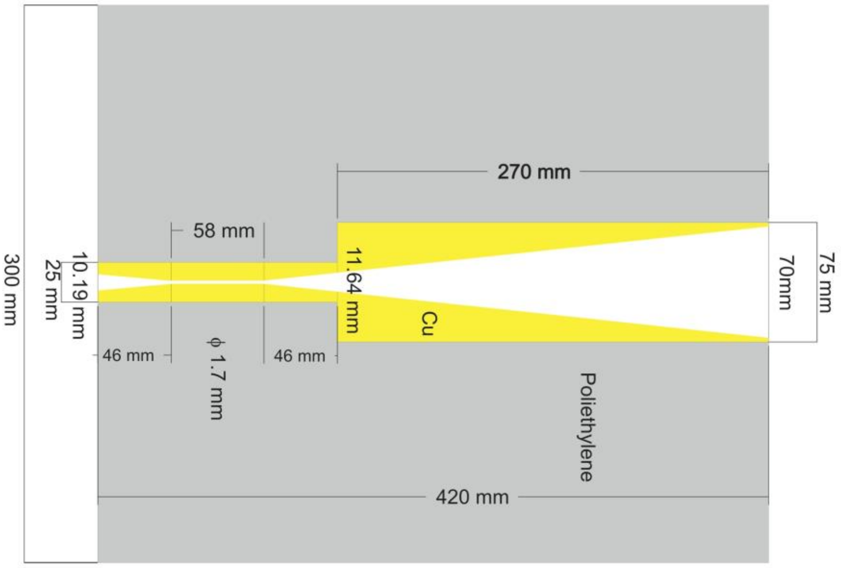

Fig. 8. Schematic diagram of the collimator and shielding setup for the neutron pinhole camera.

The design and detailed analysis of the collimator and shielding geometry was performed by means of Monte Carlo neutron transport computations [7]. A response function of the pinhole collimator was calculated using the MCNP code [8].

Various configurations of the neutron source has been used in the MCNP calculations. In this paper the results are presented for two cases:

1) The isotropic neutron point source with 2.5 MeV energy. In this case the source was located on the axis of the setup as it is presented in Fig. 9. The result of these calculations is presented in Fig. 11.

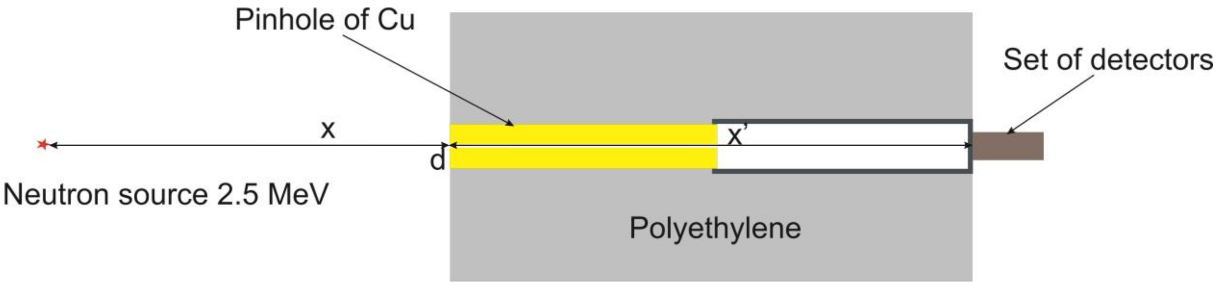

Fig. 9. Schematic diagram for the neutron pinhole camera with at a point neutron source.

2) The neutron source composed of five point sources, 2.45 MeV, with the same intensity, spread in a line at the distances 0, 0.5, 1.0, 1.5 and 2.0 cm from the axis of the pinhole (Fig. 10). A result of the corresponding calculation is presented in Fig. 12.

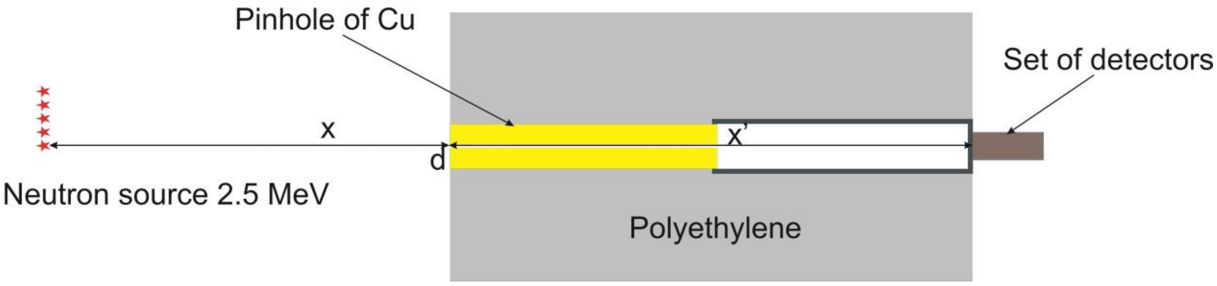

Fig. 10. Schematic diagram for the neutron pinhole camera at a five-point neutron source.

The result of the calculations was the number of neutrons entering the detectors across their forehead surfaces. In the MCNP, the Tally cards are used to specify which type of information the user wants to gain from the Monte Carlo calculation. The input data to these cards are used to describe tally "bins", a subdivision of the tally space into discrete and contiguous increments, such as cosine (corresponding to the angle), energy, or time. In the calculations performed, the Surface Tally Type (f1) for neutrons was used. The result of the calculations was the neutron current crossing a surface (number of neutrons / 1 cm^2 / source particle). Neutrons cross the surfaces that form foreheads of the detectors. The interesting part of this surface was divided into 41 pieces and neutron current was calculated across the 1×1 mm^2 pixels of the surface. The Cosine Card was used to obtain the neutron current flowing only into the detector. This card causes that the current is calculated within specified angular bins. The angular bins are defined with respect to the normal to the surface In the presented calculations the angles were assumed between 0° and 90°. It is essential to register only neutrons which come directly from the source (i.e. with the energy equal to the neutron source energy). For the purpose the Energy Card was used, and Tally was also divided into the energy bins. Tally was scored in 6 energy bins (0 – 0.1, 0.1 – 0.5, 0.5 – 1, 1 – 2, 2 – 2.5 MeV, and the last bin for a sum of all energy neutrons).

Figures 11 and 12 show examples of the response function (neutrons / 1 cm^2 / source neutron) for a point source placed on the axis of the collimator and for a five-point source located symmetrically with respect to the axis. The following parameters of the pinhole were assumed:

Material: Cu;
Length: 15 cm (46+58+46 mm), cf. Fig. 8;
Diameter: 0.17 cm;
Neutron energy: all.

The results were obtained for $2 \cdot 10^9$ neutrons emitted from the source.

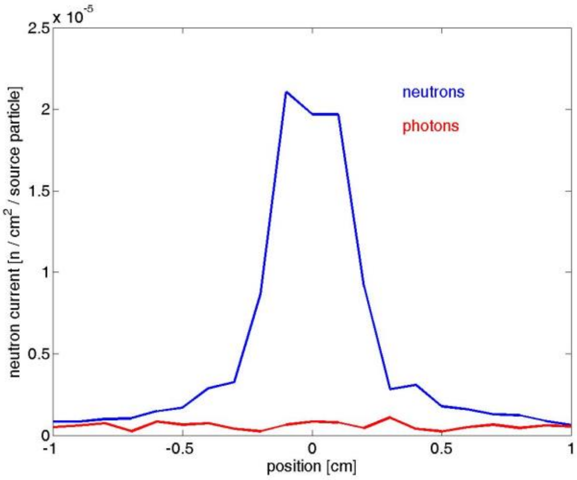

Fig. 11. Response function of the 0.17 cm pinhole, for a point source located on axis, calculated with MCNP.

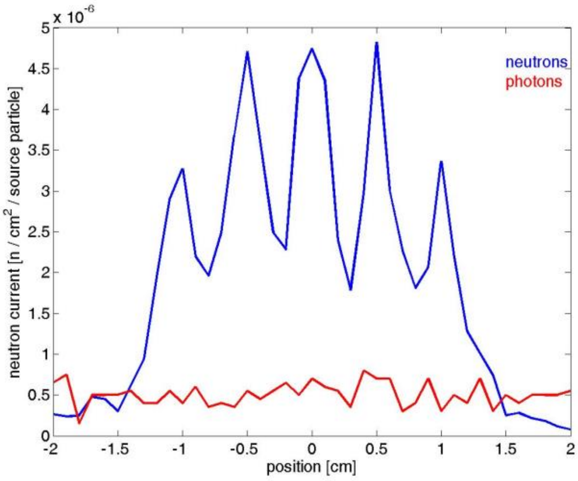

Fig. 12. Response function of the 0.17 cm pinhole, for a five point-source (located symmetrically to the pinhole axis), calculated with MCNP.

Fig. 11 illustrates that for a point object on axis, a shape cut off is observed with the background less than 15 %.Thus, cross-talk exists between adjacent resolution elements as shown in Fig. 9. In Fig 12, an image of five-point source is well represented although the observed neutron intensity from the points farthest from the axis is lower.

It is obvious that the Monte Carlo calculations (MCNP) must be taken into account in the design of the shield and the collimator pinhole camera. It is very important to obtain a low radiation background and cross-talk between adjacent elements.

6. Detectors

A neutron imaging system should be planned in the image plane of the pinhole camera. Before describing specific detection system, a general discussion of the sensitivity requirements and overall geometry should be performed. A detection system with a very high efficiency must be used in order to detect an image fluence of 100 neutrons/cm^2 and relate it to neighbouring regions where the fluence may be one order lower or higher. This suggests to use scintillators arranged in a matrix and/or a line array with a thickness of the order of the neutron mean free path. Since the scintillators are connected to the photo-multiplier tubes (PMT) the time-resolved measurements can be carried out. It gives an opportunity to separate hard X-ray and/or gamma-ray radiation from neutrons produced in the PF-24 device for a corresponding source to detector distance.

The individual scintillator should be coupled optically through a long (about 25 m) plastic fibre-optic cable to PMT. It means that the detection region will be separated from the photomultiplier tubes area. Thus, the individual scintillators will be assembled at the image plane of the camera as a closely packed line matrix array. Initially, the neutron pinhole camera will consist of four scintillators arranged in a line matrix. The final version of the camera will contain eight detectors. Since the geometrical layout of the assembled scintillators in the image plane is known, a time dependent history of the neutron flux on each detector can be used to reconstruct the time dependent picture of the fusion reaction areas into hot plasma. It is clear that this multi-element scintillator-photomultiplier system can be very useful neutron imaging instrument with a good time resolution.

7. Conclusions

A project of the pinhole camera design for imaging sources of fusion neutrons emitted from the PF-24 pinch plasma with a spatial resolution of 0.5 cm at the source has been developed. This final design of the neutron pinhole camera will be dedicated to plasma experiments on PF-24 and will be able to image a 2 cm source, emitting neutrons on the 10^9 order, for initial version (four detectors) and a 4 cm source (eight detectors) for the final version. A time resolution of about 5 ns will be achieved for the line matrix detection system.

An image recording system will be developed to the level where quantitative flux measurements can be carried out. It will consist of eight element scintillator-photomultiplier system having the time resolution of about 1 ns and moderate spatial resolution limited by pinhole design and the number of elements.

The pinhole geometry has been tested to reduce neutron scattering to a minimum and to yield about 0.5 cm spatial resolution. The 1:1 magnification was found to be a good compromise when considering detector dimension and reasonable statistics with an efficiency of the detector. However, this magnification and distance between the pinhole and neutron source should be less than 50 cm (see Fig. 7). It means that in the arrangements we will not be able to discriminate gammas and neutrons by the time of flight method. This problem can be solved by a Pb and Bi shielding over the line matrix detection system.

The neutron pinhole camera as described in the report can be a reliable and versatile tool in investigations of dense plasma compression phenomena.

References

[1] P. Cloth, H. Conrads, *Neutronics of a dense-plasma focus-an investigation of a fusion plasma*, Nucl. Sci. Eng. **62** (1977) 675.

[2] A. Bernard, P. Cloth, et al., *The dense plasma focus – a high intensity neutron source*, Nucl. Instrum. Meth. **145** (1977) 191.

[3] K. Steinmetz, K. Hubner et al., *Neutron pinhole camera investigations on temporal and spatial structures of plasma focus neutron source*, Nucl. Fusion, **22** (1982) 25.

[4] H. Schmidt, P. Kubeš, et al., *Neutron emission characteristics of pinched dense magnetized plasmas*, IEEE Trans. Plasma Sci. **34** (2006) 2363.

[5] L. Mitchel, K. Schonbach, et al., *Neutron emission from a small 1 kJ plasma focus*, Appl. Phys. Lett. **24** (1974) 57.

[6] M. Scholz, *Plasma-Focus and controlled thermonuclear fusion*, Rpt. IFJ PAN, Kraków, ISBN 978-83-63542-24-5, 2014, www.ifj.edu.pl/publ/hab (in Polish).

[7] U. Wiącek, *Optimization of the design of the fast neutron imaging pinhole camera at the PF-24 Plasma Focus device – Monte Carlo modelling.* Rept. IFJ (2014, in preparation).

[8] X-5 Monte Carlo Team, *MCNP – A general Monte Carlo N-particle transport code, Version 5.* Los Alamos National Laboratory, LA-UR-03-1987 (2008).